Human Reproduction, Vol.29, No.3 pp. 555–567, 2014
Advanced Access publication on November 27, 2013 doi:10.1093/humrep/det422

human reproduction

ORIGINAL ARTICLE ***Reproductive biology***

Dopamine in human follicular fluid is associated with cellular uptake and metabolism-dependent generation of reactive oxygen species in granulosa cells: implications for physiology and pathology

S. Saller[1], L. Kunz[2], D. Berg[3], U. Berg[3], H. Lara[4], J. Urra[4], S. Hecht[5], R. Pavlik[5], C.J. Thaler[5], and A. Mayerhofer[1,*]

[1]Anatomy III—Cell Biology, Ludwig Maximilian University Munich, Munich, Germany [2]Division of Neurobiology, Department of Biology II, Ludwig Maximilian University Munich, Munich, Germany [3]ART, Bogenhausen, Munich, Germany [4]Laboratorio de Neurobioquimica, Facultad de Quimica y Ciencias Farmaceuticas, Universidad de Chile, Santiago, Chile [5]Gynecological Endocrinology and Reproductive Medicine, Department of Gynecology and Obstetrics, Klinikum Ludwig Maximilian University, Munich, Germany

*Correspondence address. Tel: +49-89-4140-3150; Fax: +49-89-397035; E-mail: mayerhofer@lrz.uni-muenchen.de

Submitted on July 1, 2013; resubmitted on October 21, 2013; accepted on October 28, 2013

STUDY QUESTION: Is the neurotransmitter dopamine (DA) in the human ovary involved in the generation of reactive oxygen species (ROS)?

SUMMARY ANSWER: Human ovarian follicular fluid contains DA, which causes the generation of ROS in cultured human granulosa cells (GCs), and alterations of DA levels in follicular fluid and DA uptake/metabolism in GCs in patients with polycystic ovary syndrome (PCOS) are linked to increased levels of ROS.

WHAT IS KNOWN ALREADY: DA is an important neurotransmitter in the brain, and the metabolism of DA results in the generation of ROS. DA was detected in human ovarian homogenates, but whether it is present in follicular fluid and plays a role in the follicle is not known.

STUDY DESIGN, SIZE AND DURATION: We used human follicular fluid from patients undergoing in vitro fertilization (IVF), GCs from patients with or without PCOS and also employed mathematical modeling to investigate the presence of DA and its effects on ROS.

PARTICIPANTS/MATERIALS, SETTING AND METHODS: DA in follicular fluid and GCs was determined by enzyme-linked immunosorbent assay. GC viability, apoptosis and generation of ROS were monitored in GCs upon addition of DA. Inhibitors of DA uptake and metabolism, an antioxidant and DA receptor agonists, were used to study cellular uptake and the mechanism of DA-induced ROS generation. Human GCs were examined for the presence and abundance of transcripts of the DA transporter (DAT; SLC6A3), the DA-metabolizing enzymes monoamine oxidases A/B (MAO-A/B) and catechol-*O*-methyltransferase and the vesicular monoamine transporter. A computational model was developed to describe and predict DA-induced ROS generation in human GCs.

MAIN RESULTS AND ROLE OF CHANCE: We found DA in follicular fluid of ovulatory follicles of the human ovary and in GCs. DAT and MAO-A/B, which are expressed by GCs, are prerequisites for a DA receptor-independent generation of ROS in GCs. Blockers of DAT and MAO-A/B, as well as an antioxidant, prevented the generation of ROS ($P < 0.05$). Agonists of DA receptors (D1 and D2) did not induce ROS. DA, in the concentration range found in follicular fluid, did not induce apoptosis of cultured GCs. Computational modeling suggested, however, that ROS levels in GCs depend on the concentrations of DA and on the cellular uptake and metabolism. In PCOS-derived follicular fluid, the levels of DA were higher ($P < 0.05$) in GCs, the transcript levels of DAT and MAO-A/B in GCs were 2-fold higher ($P < 0.05$) and the DA-induced ROS levels were found to be more than 4-fold increased ($P < 0.05$) compared with non-PCOS cells. Furthermore, DA at a high concentration induced apoptosis in PCOS-derived GCs.

LIMITATIONS, REASONS FOR CAUTION: While the results in IVF-derived follicular fluid and in GCs reveal for the first time the presence of DA in the human follicular compartment, functions of DA could only be studied in IVF-derived GCs, which can be viewed as a cellular model

for the periovulatory follicular phase. The full functional importance of DA-induced ROS in small follicles and other compartments of the ovary, especially in PCOS samples, remains to be shown.

WIDER IMPLICATIONS OF THE FINDINGS: The results identify DA as a factor in the human ovary, which, via ROS generation, could play a role in ovarian physiology and pathology. The results obtained in samples from women with PCOS suggest the involvement of DA, acting via ROS, in this condition.

STUDY FUNDING/COMPETING INTERESTS: This work was supported by a grant from DFG MA1080/17-3 and in part MA1080/19-1. There are no competing interests.

Key words: ovary / signaling / catecholamine / computational model / polycystic ovary syndrome

Introduction

Dopamine (DA) is an important brain neurotransmitter, which is involved, for example, in Parkinson disease and psychiatric disorders (Nemeroff and Bissette, 1988; Sulzer and Schmitz, 2007; Surmeier, 2007) and acts via D1- and D2-like receptors (Missale *et al.*, 1998). DA is metabolized by monoamine oxidases A/B (MAO-A/B) and catechol-*O*-methyltransferase (COMT; Perfeito *et al.*, 2012). COMT is membrane-bound, while MAO enzymes are localized within the cell in mitochondria (Goldstein *et al.*, 2003) and DA metabolism by MAO thus requires its cellular uptake.

In the course of the intracellular metabolic breakdown of monoamines, including DA, aldehydes and hydrogen peroxide (H_2O_2) are produced. H_2O_2 is an important member of the class of reactive oxygen species (ROS). ROS can exert both nocuous and beneficial effects (Finkel, 2011; Shkolnik *et al.*, 2011), depending on the levels. High levels of ROS can induce lipid peroxidation, an action described to occur as a consequence of the metabolism of DA in astrocytes (Vaarmann *et al.*, 2010). An imbalance between abundant ROS levels and the antioxidant systems can also result in severe cell damage and apoptosis (Finkel, 2011). DA appears to contribute in this way to neuronal cell death in Parkinson disease (Perfeito *et al.*, 2012).

ROS are also generated in the ovary, and a recent study in human granulosa cells (GCs) implicated the neurotransmitter norepinephrine (NE) in the generation of ROS (Saller *et al.*, 2012). NE, presumably derived from sympathetic fibers innervating the wall of follicles and the circulation, was found in follicular fluid of women undergoing in vitro fertilization (IVF). NE was taken up into cultured human GCs via a transporter (NET; SLC6A2) and was metabolized via mitochondrial MAO-A (Eisenhofer *et al.*, 1995; Goldstein *et al.*, 2003; Saller *et al.*, 2012) in GCs. Functional uptake of NE and expression of MAO were also found in rat GCs (Greiner *et al.*, 2008).

In addition to abundant levels of NE, DA was also detected in human ovarian homogenates (Lara *et al.*, 2001). D1- and D2-like receptors were described in the follicle and the corpus luteum, and their functionality was tested in isolated human GCs. GCs express the D1-like receptor types D1 and D5, which are G-protein-coupled and linked to cAMP increase, and the D2-like receptor types D2 and D4, which are linked to IP3/DAG. D3 was not found (Rey-Ares *et al.*, 2007). Indeed, by monitoring cAMP or intracellular Ca^{2+}, the functionality of D1- and D2-like receptors could be shown (Mayerhofer *et al.*, 1999, 2000, 2004; Rey-Ares *et al.*, 2007). In addition to the receptors for DA, the cell membrane-associated DA transporter (DAT) was found in rat and human GCs and in monkey oocytes (Mayerhofer *et al.*, 1998; Greiner *et al.*, 2008). Oocytes, but no other ovarian cell type, express the enzyme DA hydroxylase (DBH) and under experimental conditions can take up DA and convert it to NE (Mayerhofer *et al.*, 1998). Hence, a complex ovarian DA system, which includes receptor-mediated roles for DA and DA metabolism, may be assumed. Yet, it remains to be shown whether DA in sufficiently high concentrations is indeed present in the follicular compartment and in the follicular fluid. If so, the question arises of whether ovarian DA could also be further metabolized in the follicle and if this may lead to ROS generation.

In view of recent publications, this point appears of interest. A report described DA metabolism in human GCs and the results showed increased metabolism of DA in GCs derived from women suffering from the common human ovarian pathology, polycystic ovary syndrome (PCOS; Gómez and Ferrero, 2011). In PCOS, affecting up to 10% of women of reproductive age, there is ample evidence for increased follicular ROS levels and oxidative stress (Ehrmann, 2005; Stener-Victorin *et al.*, 2009; Qiao and Feng, 2011). This includes significantly elevated ROS levels in individual cultured GCs derived from PCOS patients (Karuputhula *et al.*, 2013). Finally, there is evidence for alterations in mitochondrial function in PCOS women and for alterations in catecholamine metabolism (Nemeroff and Bissette, 1988; Garcia-Rudaz *et al.*, 1998; Victor *et al.*, 2009).

In this study, we explored whether DA is a factor in the human follicular fluid and may cause the generation of ROS. We studied DA levels in follicular fluid and GCs, determined the uptake, metabolism and consequences in GCs as well as established a computational model of these processes to predict potential consequences in GCs from PCOS- and non-PCOS patients.

Materials and Methods

Samples

DA levels were determined in the follicular fluid of 20 women with regular menstrual cycles undergoing IVF (with or without ICSI) because of male infertility, and in follicular fluid from 19 lean PCOS patients (Saller *et al.*, 2012). The body mass index (BMI) and the age range of both groups were comparable (means $\pm$ SD: 23.0 $\pm$ 3.9 kg/m^2 versus PCOS, 22.5 $\pm$ 3.8 kg/m^2; 32.7 $\pm$ 4.2 year versus PCOS, 33.1 $\pm$ 4.2 year). All samples are aliquots of those which we previously used to measure NE, and all had been treated in the same way, i.e. they had been thawed twice prior to the determination of DA. The diagnosis of PCOS was based on the Rotterdam criteria (Revised 2003 consensus on diagnostic criteria and long-term health risks related to polycystic ovary syndrome (PCOS) 2004). As mentioned previously (Saller *et al.*, 2012), a standard gynecological examination including a transvaginal

sonography was performed. Patients displaying signs or symptoms of anomalies including uterine fusion defects, submucosal fibroids or acute inflammation were excluded. There was no evidence of thyroid dysfunction or hyperprolactinemia. Approval was obtained from the local ethics committee. All participants gave their written informed consent and samples were anonymized. The 'long' protocol was used (Acharya *et al.*, 1992) and included treatment (nasal spray) with the GnRH agonist nafarelin (Synarela®, Pharmacia GmbH, Karlsruhe, Germany). When pituitary downregulation was confirmed [luteinizing hormone (LH) <5 mIU/ml and E2 <50 pg/ml], ovarian stimulation was started (recombinant FSH; Puregon®, Essex Pharma GmbH, Munich, Germany). When greater than or equal to three follicles reached a mean diameter of at least 17 mm, 250 μg of recombinant hCG (Ovitrelle®, Serono GmbH, Unterschleißheim, Germany) were administered s.c. Oocyte retrieval was performed under general anesthesia by transvaginal, ultrasound-guided aspiration 35 h later. After obtaining the oocytes, follicular fluids from one woman were pooled, immediately centrifuged for 10 min at 1000*g* and supernatants were stored at -70°C. Samples with visible blood or flushing fluid contamination were excluded.

ELISA measurements of DA

DA was determined using an enzyme-linked immunosorbent assay (ELISA) kit (DRG Diagnostics, Marburg, Germany), following the instructions of the manufacturer. The catecholamines were first extracted by using a cis-diolspecific affinity gel, acylated and then converted enzymatically. Measurements were performed in microtiter plates, and reactions were monitored at 450 nm in a plate-reading luminometer (BMG LABTECH GmbH, Fluostar, Offenburg, Germany). DA in the range of 0.5 ng/ml–5 μg/ml (3.3 nM – 32.7 μM) can be detected with this assay. Values below the detection limit were classified as not detectable.

GC culture studies

For all other experiments with GCs, including uptake experiments, follicular fluid containing GCs was derived from additional IVF patients ($n = 56$) stimulated according to routine protocols. They included patients with PCOS ($n = 19$), but the PCOS and non-PCOS groups of patients were not matched for BMI or age. Aspirates with cells from 2 to 4 patients were pooled for each experiment. GCs were separated by centrifugation at 560*g* for 3 min, washed in serum-free DMEM/Ham's F-12 medium (Sigma, Munich, Germany) and suspended in culture medium supplemented with penicillin (100 U/ml), streptomycin (100 μg/ml) and 10% fetal calf serum (Gibco, Berlin, Germany), as previously described (Saller *et al.*, 2010, 2012). DA, Nomifensine (Nf), *N*-acetylcysteine (NAC) and SKF38393 were purchased from Sigma and dissolved in H_2O to a 1-mM stock concentration. U-91,356A and MAO-A/B inhibitors, 8-(3-chlorostyryl) caffeine and pirlindole mesylate, were purchased from BIOZOL (Eching, Germany) and were dissolved in dimethyl sulfoxide (DMSO). For cellular studies, DMSO was added to the respective controls, and final concentrations were <0.0001%.

RT–PCR and quantitative (q)RT–PCR

Total RNA from several batches (at least five for each parameter) of cultured GCs (2 days after isolation) was prepared using the peqGold Total RNA Kit (Peqlab, Erlangen, Germany), as described (Rey-Ares *et al.*, 2007). In brief, total RNA (200–500 ng) was subjected to reverse transcription, using random primers (pdN6) and SuperScript II Reverse Transcriptase, 200 U/μl (Invitrogen GmbH, Darmstadt, Germany). Commercial human brain and ovary cDNAs (BD CLONTECH, Inc., Heidelberg, Germany) were also used as controls. PCR steps consisted of 35 cycles of denaturing (at 94°C for 60 s), annealing (at 60°C for 30 s) and extension (at 72°C for 60 s). Reaction tubes lacking reverse transcription product or RNA were used as PCR controls. The identities of all PCR products were verified by direct sequencing using one of the specific primers. Oligonucleotide primers were designed to span at least one intron (Table I). Amplification of cDNAs for qRT–PCR was performed employing the Quantifast SYBR Green qRT–PCR kit (Quiagen, Hilden, Germany). The StepOnePlus™ Real-Time PCR system (AB applied biosystems by life technologies) for continuous fluorescent detection was used. Samples and standards were amplified in triplicate. The levels were normalized to the ubiquitine (UQ) housekeeping gene (Adam *et al.*, 2012a,b).

Measurement and quantification of ROS

The 2-,7-dichlorodihydrofluoresceindiacetate ($DCFH_2$-DA) method was used, as described (Schell *et al.*, 2010; Saller *et al.*, 2012). In the presence of intracellular ROS, such as H_2O_2, the $DCFH_2$-DA dye (Invitrogen, Karlsruhe, Germany), after intracellular ester hydrolysis, is converted to the highly fluorescent compound DCF. GCs seeded on glass cover slips at subconfluence were stimulated for up to 2 h with or without DA. Cells were washed with phosphate-buffered saline (10 mM, pH 7.4) and then transferred to extracellular fluid buffer containing 140 mM NaCl, 3 mM KCl, 1 mM $MgCl_2$, 1 mM $CaCl_2$, 10 mM HEPES and 10 mM glucose (pH 7.4) and $DCFH_2$-DA (10 μM) for 30 min loading at 37°C. DCF fluorescence was measured at 485 nm excitation/520 nm emission, monitored by fluorescence microscopy (Zeiss Axioskop FSZ+). For quantification of ROS, GCs were placed in 96-well plates, treated with extracellular fluid buffer and then with 100 nM DA/10 μM Nf/1 mM NAC/10 nM MAO-A/B inhibitor/1 μM SKF38393, 1 μM U-91,356A and $DCFH_2$-DA. Fluorescence levels were measured in a fluorimeter at room temperature (BMG LABTECH GmbH). After 2 h, when the experiments were terminated, the final values were statistically analyzed. Fluorescence intensities were normalized to controls.

Viability and caspase assays

Cellular ATP levels, as a measure of cellular viability, were studied using the CellTiter-Glo Luminescent Cell Viability Assay (Promega, Mannheim, Germany). The activity of the effector caspase 3/7, as a measure of apoptotic cell death, was studied using a caspase 3/7 assay (Promega), as described (Saller *et al.*, 2010). For ATP and caspase measurements, GCs on Day 3 of culture were used.

Statistical analyses

Data were analyzed using Prism 4 (GraphPad Software, San Diego, CA, USA). Results of ELISA measurements of DA were examined by the *F*-test revealing equal variances ($P = 0.1056$). Additionally, the data passed two normality tests, Kolmogorov–Smirnov and Dostino and Pea, Kolmogorov–Smirnov and D 'Agostino and Pearson test, respectively. Hence, we considered that application of a *t*-test is valid. The Student's *t*-test was used to analyze the results from qRT–PCR studies. For analyses of the other results, we used one-way analysis of variance (ANOVA) followed by the Newman–Keuls test or two-way ANOVAs and Bonferroni *post hoc* test, as indicated.

Computational model

The model is mainly based on modeling data related to the function of DA as neurotransmitter (Justice *et al.*, 1988; Nicolaysen and Justice, 1988; Qi *et al.*, 2008; Best *et al.*, 2009, 2010). We considered nine differential equations as described below in our model and solved them numerically by means of the software COPASI 4.8 (Hoops *et al.*, 2006; Best *et al.*, 2009). The reactions follow either first-order or Michaelis–Menten (MM) kinetics as stated for each reaction with the kinetic parameters given in brackets. The values of these parameters as well as concentrations used in our model can be found in Table II. Extracellular DA is assumed to be taken up by DAT in a reversible way (MM kinetics; V_{max}(in), V_{max}(out), K_m(in), K_m(out)). This transport can be inhibited by Nf; K_i(Nf). Intracellular DA is converted to

Table I Oligo-deoxynucleotide primers used in RT–PCR experiments.

Type	Primer sequence (5′–3′)	GenBank accession number
DAT-sense	AGC CGG CAC GTC CAT CCT CTT TG	NM_001044
DAT-antisense	GGC GCA CCT CCC CTC TGT CCA C	NM_001044
DAT-nested-antisense	ATG CTG ACC ACG ACC ACG A	NM_001044
DAT-qPCR-sense	ACG GTG GCA TCT ACG TCT TC	NM_001044
DAT-qPCR-antisense	CAC CAT AGA ACC AGG CCA CT	NM_001044
MAO-A-qPCR-sense	CCA TCA TGG GCT TCA TTC TT	NM_000240.3
MAO-A-qPCR-antisense	GAT CCC AGC ACT TTG GCA TA	NM_000240.3
MAO-B-sense	TAT GTG AT TAGT GCT ATT CCT CCT A	NM_000898
MAO-B-antisense	ACT TGA GAT ACG GTT CCA AGA C	NM_000898
MAO-B-qPCR-sense	GAT TTA TCC TGG CCC ACA AA	NM_000898
MAO-B-qPCR-antisense	GCT CCA GAG CTT CTA GGG AAC	NM_000898
COMT-qPCR-sense	GTC GCG GGA GAG AAA TAA CA	NM_000754
COMT-qPCR-antisense	GGC ATC TTC AAA GCA CCT CT	NM_000754
COMT-sense	TGG ACG CCG TGA TTC AGG AG	NM_000754
COMT-antisense	CCT CGC AGG GTC CTG TAG TAG	NM_000754
VMAT2-qPCR-sense	TTG TGC TCT TCT GGG AAT	NM_003054.4
VMAT2- qPCR-antisense	CCA ATT GCA AAA CCA ACT	NM_003054.4
UQ-198-sense	AGA TCC AGG ATA AGG AAG GCA T	NM_021009.5
UQ-198-antisense	GCT CCA CCT CCA GGG TGA T	NM_021009.5

DAT, DA transporter; MAO-A, monoamine oxidase A; MAO-B, monoamine oxidase B; COMT, catechol-*O*-methyltransferase; VMAT2, vesicular monoamine transporter; UQ-198, ubiquitine.

3,4-dihydroxyphenylacetic acid (DOPAC) and H_2O_2 in a reaction, catabolized by MAO, which follows MM kinetics (V_{max}(MAO/DA), K_m(MAO/DA)) and can be inhibited by MAO inhibitors (K_i(MAO)). As shown in our experiments, there are two MAO forms, MAO-A and -B, with differing kinetics and pharmacology. However, as these differences are not in the range of orders of magnitude and since there are no data available on ovarian MAO kinetics, we did not distinguish between the two forms in our model. Intracellular DA is also metabolized in a COMT-catalyzed reaction to 3-methoxytyramine (3-MT) with MM kinetics (V_{max}(COMT/DA) and K_m(COMT/DA)). Both enzymes catalyze also further reactions. 3-MT is transformed by MAO yielding homovanillic acid (HVA) by first-order kinetics (k_{MAO}(3MT)), which can be blocked as well (K_i(MAO)). COMT metabolizes DOPAC producing HVA and $O_2^{\cdot-}$ with first-order kinetics (k_{COMT}(DOPAC)). In a final metabolizing step, HVA is assumed to be removed by a first-order kinetics reaction ($k_{HVA\text{-}catabolism}$). In summary, ROS are assumed to be produced during metabolism of DA by MAO (H_2O_2) and of DOPAC by COMT ($O_2^{\cdot-}$). Superoxide dismutase (SOD) is transforming $O_2^{\cdot-}$ to H_2O_2 following first-order kinetics (k_{SOD}). H_2O_2 is removed from the system by conversion to water by catalase (CAT) and glutathione peroxidase (GPX) in reactions that follow first-order kinetics (k_{CAT} and k_{GPX}, respectively). For the ovary, no biochemical data on kinetics of DA metabolism are available, and we have, thus, to rely mainly on neuronal values. We ran our model not only with the values in Table II, but also with varying parameters to test for robustness of the model. Either, we varied the values in the range given in the literature or, if only one value was published, we used values ranging from one-third to three times the value published. For GCs from PCOS patients, a similar model was established and values differing from those for non-PCOS GCs can be found in Table II. Based on our qRT–PCR data, we assumed that the doubled expression levels of mRNA encoding DAT, MAO-A and -B translated in doubled enzymatic activity. Therefore, the corresponding V_{max} values for MM kinetics or *k*-values for first-order kinetics were multiplied by two. Extracellular DA concentrations have been chosen according to our experimental conditions, i.e. 5 μM for uptake simulations, 10 and 100 nM, respectively, for modeling of ROS generation, and the concentrations found in follicular fluid (Fig. 1; 60 nM for non-PCOS and 120 nM for PCOS) for simulation of physiological conditions. Concentrations of DAT and MAO inhibitors have been determined to equal those used in our experiment. All other concentrations have been set to be variable with a starting value of zero.

Results

DA is present in human follicular fluid and in GCs: differences between PCOS and non-PCOS samples

DA was detected at variable levels in follicular fluid from most PCOS and non-PCOS women. For the non-PCOS group, the levels ranged from not detectable (<3.3 nM) to 213.2 nM (mean: 58.04 nM; median 45.75 nM, 25% percentile 0.0, 75% percentile 107.6; $n = 20$). In the PCOS group, DA ranged from not detectable (<3.3 nM) to 268.0 nM (mean: 116.9 nM; median 119.7, 25% percentile 30.07, 75% percentile 187.1; $n = 19$) (Fig. 1A and Supplementary data, Table S1). Thus, significantly lower levels of DA were measured in follicular fluid of women undergoing IVF for male infertility than in those from PCOS patients ($P = 0.0309$; *t*-test).

Freshly isolated human GCs also contained traces of DA in the range of not detectable to 1.03 nM/μg protein (not detectable–1.8 pg/μg

Table II Kinetic parameters used in our computational model.

Reaction	Parameter	Model value	References
DAT	V_{max}(in)/μM min^{-1}	100	Nicolaysen and Justice (1988); Gu *et al.* (1994); Lingjaerde *et al.* (1981); Chen and Justice (2000); Best *et al.* (2009)
	V_{max}(out)/μM min^{-1}	200	Nicolaysen and Justice (1988); Gu *et al.* (1994); Lingjaerde *et al.* (1981); Chen and Justice (2000); Best *et al.* (2009)
	K_m(in)/μM	10	Nicolaysen and Justice (1988); Gu *et al.* (1994); Lingjaerde *et al.* (1981); Chen and Justice (2000); Best *et al.* (2009)
	K_m(out)/μM	10	Nicolaysen and Justice (1988); Gu *et al.* (1994); Lingjaerde *et al.* (1981); Chen and Justice (2000); Best *et al.* (2009)
	K_i(Nf)/μM	0.1	Nicolaysen and Justice (1988); Gu *et al.* (1994); Lingjaerde *et al.* (1981); Chen and Justice (2000); Best *et al.* (2009)
DAT (PCOS)	V_{max}(in, PCOS)/μM min^{-1}	200	Values doubled[a]
	V_{max}(out, PCOS)/μM min^{-1}	400	Values doubled[a]
MAO	V_{max}(MAO/DA)/μM min^{-1}	15	Houslay and Tipton (1974); O'Carroll *et al.* (1986); Fernández de Arriba *et al.* (1991); Best *et al.* (2009)
	K_m(MAO/DA)/μM	300	Houslay and Tipton (1974); O'Carroll *et al.* (1986); Fernández de Arriba *et al.* (1991); Best *et al.* (2009)
	K_i(MAO)/μM	0.2	Chen *et al.* (2002); Petzer *et al.* (2003); Vlok *et al.* (2006)
	k_{MAO}(3MT)/min^{-1}	0.3	Justice *et al.* (1988)
MAO (PCOS)	V_{max}(MAO/DA, PCOS)/μM min^{-1}	30	Values doubled[a]
	k_{MAO}(3MT, PCOS)/min^{-1}	0.6	Values doubled[a]
COMT	V_{max}(COMT/DA)/μM min^{-1}	3	Best *et al.* (2009)
	K_m(COMT/DA)/μM	0.5	
	k_{COMT}(DOPAC)/min^{-1}	0.038	Justice *et al.* (1988)
HVA catabolism	$k_{HVA\text{-}catabolism}$/$min^{-1}$	0.0575	Best *et al.* (2009)
SOD	k_{SOD}/min^{-1}	200 000	Riley *et al.* (1991); Bolann *et al.* (1992); Goldstein *et al.* (2006); Kowald *et al.* (2006); BRENDA
CAT	k_{CAT}/min^{-1}	3000	Kowald *et al.* (2006); BRENDA
GPX	k_{GPX}/min^{-1}	2000	Kowald *et al.* (2006); BRENDA

in, inwards; out, outwards; DAT, dopamine transporter; MAO, monoamine oxidase; COMT, catechol-*O*-methyltransferase; PCOS, polycystic ovary syndrome; HVA, homovanillic acid; SOD, superoxide dismutase; CAT, catalase; GPX, glutathione peroxidase; 3MT, 3-methoxytyramine; DOPAC, 3,4-dihydroxyphenylacetic acid; Nf, nomifensine.
V_{max}: maximum rate of Michaelis–Menten kinetics.
K_m: Michaelis constant of Michaelis–Menten kinetics.
K_i: dissociation constant of inhibitor.
k_{MAO}(3MT): first-order rate constant of 3MT decomposition by MAO.
k_{COMT}(DOPAC) : first-order rate constant of DOPAC decomposition by COMT.
$k_{HVA\text{-}catabolism}$: first-order rate constant of HVA catabolism.
k_{SOD}: first-order rate constant of SOD.
k_{CAT}: first-order rate constant of CAT.
k_{GPX}: first-order rate constant of GPX.
[a]Values doubled based on our qRT–PCR results on mRNA expression.

protein) (median 0.006, 25% percentile 0.0, 75% percentile 0.37; $n = 12$ non-PCOS patients) (data not shown) and not detectable to 0.04 nM/μg protein (0–0.5 pg/μg protein) (median 0.0, 25% percentile 0.0, 75% percentile 0.0; $n = 8$ PCOS patients).

Expression of DAT, COMT, MAO-A and -B by human GCs and active uptake of DA

Cultured GCs from the PCOS (not shown) and non-PCOS group express the genes for DAT, COMT, MAO-A and -B, as analyzed by RT–PCR followed by sequencing (Fig. 1B).

ELISA measurements of DA in lysed GCs (at Day 3 of culture), which had been exposed to DA for 2 h, revealed that GCs take up DA from the medium. This was shown for PCOS ($n = 3$ experiments; Fig. 1D) and non-PCOS samples ($n = 3$ experiments; Fig. 1C). The specificity of the DAT-driven uptake was examined using the DAT-blocker Nf. Its ability to partially but significantly block intracellular accumulation supports the involvement of DAT (Fig. 1C and D).

Consequences of DA in human GCs: ROS generation and apoptosis

DA added in the concentration range as present in human follicular fluid (10 nM–1 μM) to cultured GCs (Day 3) caused the generation of ROS. Figure 2A gives a microscopic view of GCs treated with or without 100 nM DA for 30 min. The ROS levels increased within minutes and continued to rise until the termination of the experiments after 2 h (Fig. 3A). The treatment of GCs (Day 3 of culture; from non-PCOS

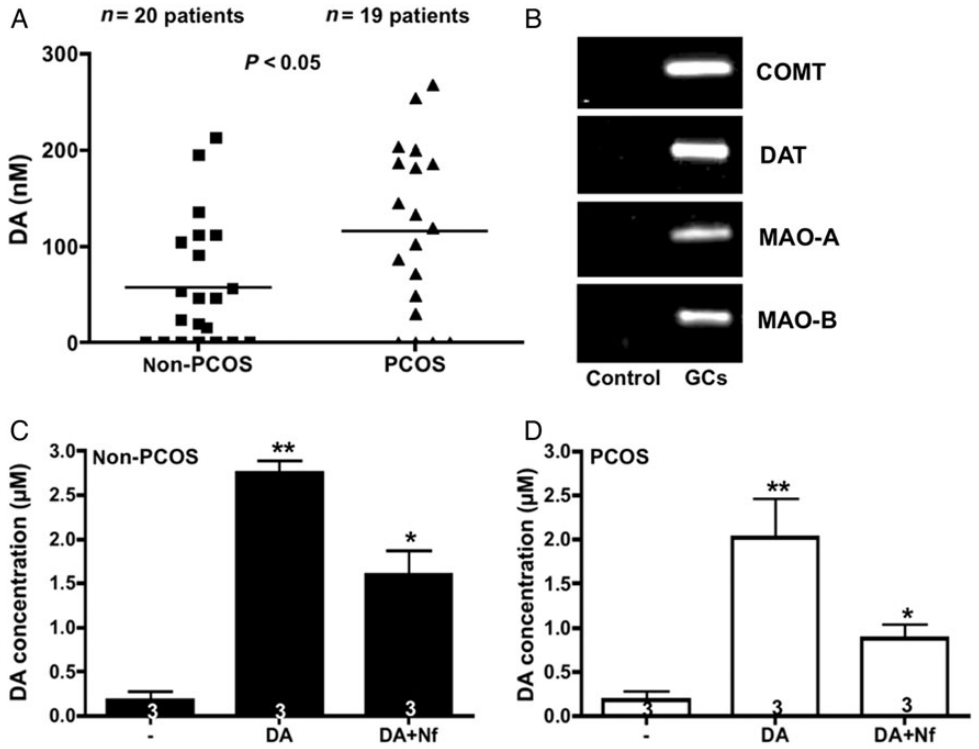

Figure 1 DA in follicular fluid of in vitro fertilization (IVF) patients and evidence for DA uptake and metabolism in GCs. (**A**) Individual levels of DA and mean values (horizontal line) in follicular fluid of 20 IVF patients with male factor infertility (non-PCOS) and 19 patients with PCOS. *t*-test, $^{*}P < 0.05$. (**B**) Agarose gel showing RT–PCR products for DAT, COMT, MAO-A and -B in human GCs from patients with male factor infertility. Sequencing proved their identities. (**C**) Isolated human GCs from non-PCOS patients take up DA (5 μM) added to the medium 2 h prior to ELISA measurements. Intracellular levels were significantly reduced when the selective DAT-blocker Nf (10 μM) was added. Values are the mean ± SEM: for DA: 2.75 ± 0.3 μM. $n = 3$ experiments, each using pooled cells from 2 to 3 patients. ANOVA, $^{*}P < 0.01$ for DA + Nf versus DA; $^{**}P < 0.001$ for control versus DA. Control cells (−) were not treated with DA. (**D**) Isolated human GCs from PCOS patients take up DA (5 μM) (left bar) added to the medium 2 h prior to ELISA measurements. Intracellular levels are significantly reduced by the selective DAT-blocker Nf (10 μM). Control cells (−) were not treated with DA. Values are the mean ± SEM: for DA: 2.03 ± 0.3 μM; $n = 3$ experiments, each using pooled cells from 2 to 3 patients. ANOVA, $^{*}P < 0.01$ for DA + Nf versus DA; $^{**}P < 0.001$ for control versus DA. COMT, catechol-*O*-methyltransferase; DA, dopamine; DAT, DA transporter; MAO, monoamine oxidase; Nf, nomifensine.

patients) with 10 nM, 100 nM, 1 μM and 10 μM DA for 24 h had no effect on effector caspases 3/7 in GCs of non-PCOS patients (Fig. 2B). DA in the range of 1–100 nM did also not change cellular ATP levels, i.e. a measure for cell viability, which was tested in additional four experiments in up to 24 h (data not shown). Thus, DA, applied at physiological and supra-physiological concentrations, does not affect the rate of spontaneously occurring apoptotic events of GCs from non-PCOS patients.

The mechanism by which DA generates ROS was further examined (Fig. 3). The addition of 100 nM DA resulted in higher levels of ROS than that of 10 nM (Fig. 3A). Treatment of GCs with the D1/D2 receptor agonists SKF38393 (for D1) and U-91,356A (for D2) had no effect on ROS generation, implying that the generation of ROS occurs by DA is a receptor-independent event (Fig. 3B). The DA-induced ROS formation was inhibited when the selective DAT-blocker Nf (10 μM) (Fig. 3C) and the MAO-B inhibitor 8-(3-chlorostyryl) caffeine (10 nM) (Fig. 3D) were added. ROS induced by 100 nM of DA was also blocked by the antioxidant NAC (1 mM) (Fig. 3E). ROS induced by 100 nM of DA was partly blocked by the MAO-A inhibitor pirlindole mesylate (10 nM) and totally blocked by a combination of MAO-A and -B inhibitors (10 nM each) (Fig. 3F). Treatment of GCs with NAC, Nf or MAO-B inhibitor alone had no effect on ROS generation (data not shown). NAC, Nf, MAO-B inhibitor and DA were not toxic for GCs at the levels employed, as seen in viability assays using cellular ATP for up to 2 h (not shown). The results allow the conclusion that cellular uptake and metabolism are required for DA to increase ROS in GCs.

Computational modeling

The model confirmed that GCs take up DA (Fig. 4B) and produce ROS, including H_2O_2, with a similar time course as in our experiments (Fig. 4A). The uptake of DA into the cytoplasm occurred to a similar extent as in the experiment (Fig. 1C and D) for both non-PCOS and PCOS GCs and can be inhibited by Nf (Fig. 4B). When calculating ROS generation with 10 and 100 nM extracellular DA, we found a higher ROS production in PCOS GCs than in non-PCOS ones (Fig. 4C), which is in accordance with our experiments (Fig. 5A). ROS production can be inhibited in the model by blocking either DA uptake (Nf) or MAO activity (Fig. 4C). When we subjected in addition the physiological concentrations of DA found in the follicular fluid, we calculated higher intracellular DA concentrations as well as higher levels of $O_2^{\cdot-}$ and H_2O_2 in

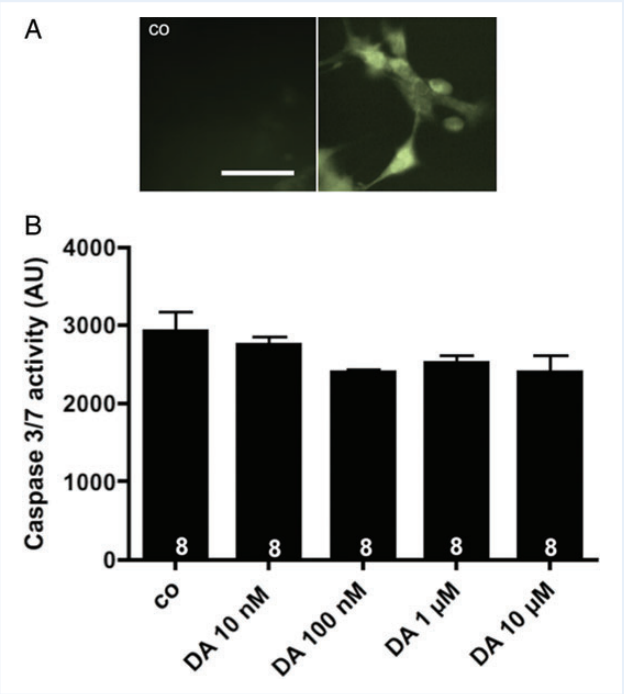

Figure 2 DA induces the generation of ROS in GCs and does not affect effector caspases 3/7. (**A**) The treatment of GCs with 100 nM DA for 30 min induces the generation of ROS, monitored by DCF fluorescence in cells. CO: same cells prior to addition of DA; bar = 60 μm. (**B**) Measurement of active effector caspases 3/7, as an indicator for apoptosis, 24 h after DA treatment of GCs from non-PCOS patients. Results are expressed in arbitrary units (AU) and are given as mean ± SEM from $n = 8$ experiments, each using pooled cells from 2 to 3 patients. The DA treatment groups are not significantly different from the control group ($P > 0.05$). DA, dopamine; ROS, reactive oxygen species; PCOS, polycystic ovary syndrome.

PCOS than in non-PCOS (Fig. 4D). All modeling results were rather robust when we varied the parameters of the model as described in the Materials and Methods sections. The ratios between values for PCOS and non-PCOS GCs were similar under all conditions.

Increased responses to DA and elevated levels of DAT, MAO-A and -B in GCs from women with PCOS

Computational modeling suggested that DA levels, its cellular uptake and metabolizing enzymes determine ROS levels in GCs. In follicular fluid of PCOS patients, 2-fold higher DA levels were found. Hence, we further tested how PCOS-derived GCs respond to DA. GCs from PCOS patients when studied in side-by-side experiments with non-PCOS GCs showed a striking, up to 5-fold increased generation of ROS caused by DA in comparison with non-PCOS cells (Fig. 5A). Furthermore, in contrast to the results obtained in non-PCOS samples, DA at high concentrations slightly but significantly induced apoptosis in PCOS-derived GCs (Fig. 5B). To study the possible causes for the enhanced ROS generation by DA, we examined the mRNA levels of DAT, MAO-A/B, COMT and the vesicular monoamine transporter 2 (VMAT2). qRT–PCR experiments revealed a significantly increased expression of MAO-B, -A and DAT mRNA in PCOS versus non-PCOS patients (Fig. 6A), but no changes in expression levels of COMT and VMAT2 mRNA (Fig. 6B). Thus, the uptake and MAO-dependent metabolism is significantly altered in PCOS, which may result in increased ROS.

Discussion

The catecholamines NE and DA are found in plasma (Van Loon, 1983) and were reported in the human ovary (Lara *et al.*, 2001). Catecholamines in any peripheral organ may be derived from the circulation and from innervation of the respective organ. In addition, tyrosine hydroxylase (TH, the rate limiting, first enzyme in catecholamine biosynthesis) immunoreactive intrinsic intraovarian neurons were described in the human ovary (Anesetti *et al.*, 2001) and may specifically contribute to ovarian catecholamines. In the same study, no other ovarian cells were described as being immunoreactive for TH. Catecholamines may exert a number of functions depending on the presence of receptors and/or, as we found, depending on cellular uptake and metabolism. Our data reveal new aspects of such a complex system involving the catecholamine DA in the human ovary.

An important pillar of this system is DA, which was detected previously in ovarian homogenate (Lara *et al.*, 2001) and now, in the present study, in follicular fluid from ovulatory follicles. The DA values measured vary, possibly because the samples were thawed before and aliquots were removed and used for another study (Saller *et al.*, 2012). Since all samples were treated in the same way, we do not consider this the main reason for variability, but rather suspect that levels may vary because of different metabolic activities *in vivo*, within follicles. In any case, the presence of DA implies that this catecholamine is to be considered a factor with the potential to influence the cells of the ovary, i.e. GCs and/or the oocyte of the large follicle. This may occur via D1- and D2-like receptors, previously found on GCs (Rey-Ares *et al.*, 2007), that are linked to the generation of cAMP, intracellular Ca^{2+} and the phosphorylation state of the third messenger DARPP32 (DA- and cAMP-regulated phosphoprotein of Mr 52). Further downstream actions of DA are not well known, but may include regulation of cell size (Mayerhofer *et al.*, 1999, 2000, 2004).

The levels of DA in follicular fluid varied substantially, and this may be related to the possibility that DA is metabolized in complex ways. DA is to be considered a precursor of follicular NE and both can be metabolized. NE and DA were, respectively, found in human ovarian homogenate (Lara *et al.*, 2001) and human follicular fluid (this study and Saller *et al.*, 2012). A previous study with non-human primate oocytes showed that oocytes take up DA and express DAT and the enzyme DBH, which converts DA to NE (Mayerhofer *et al.*, 1998). NE then targets beta-adrenergic receptors of GCs and elevates cAMP in GCs. GCs of rat and human origin (Greiner *et al.*, 2008; Saller *et al.*, 2012) can also take up and metabolize NE. In human GCs, this results in the generation of ROS (Saller *et al.*, 2012). Indeed, substantial amounts of NE (Saller *et al.*, 2012) and of a major NE metabolite 4-hydroxy-3-methoxyphenylglycol (MHPG; around 57 ng/ml) can be detected by high-performance liquid chromatography in human follicular fluid (results not shown). As in a previous study, using the same follicular fluid samples as in the present one, normetanephrine, a metabolite of DA and NE, was found in follicular fluid and also in GCs (Saller *et al.*, 2012), the combined data provide clear evidence that follicular metabolism of catecholamine occurs.

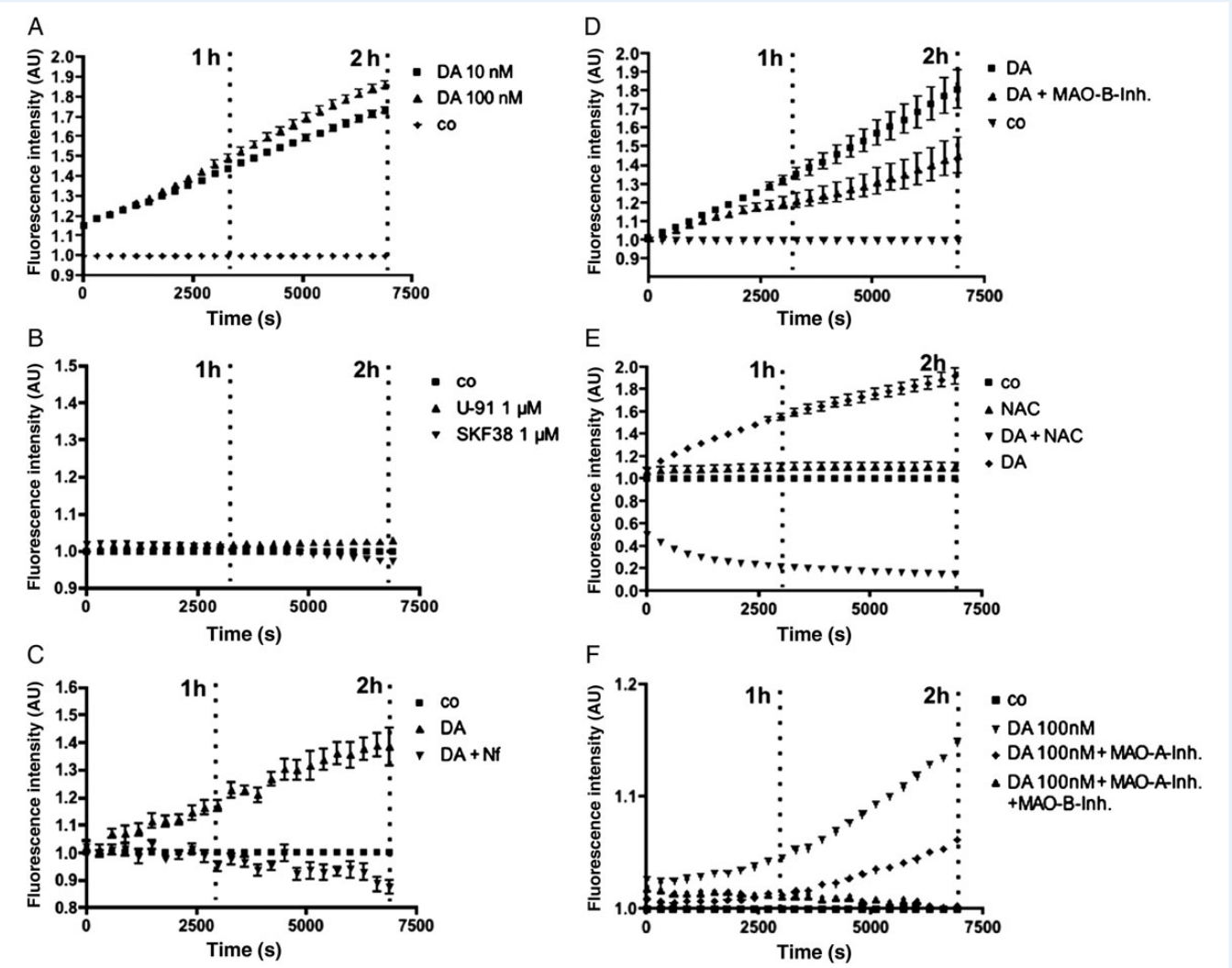

Figure 3 DA induces the generation of ROS in GCs, which can be inhibited by blockage of uptake or metabolism. (**A**) ROS levels in GCs increase upon addition of DA used at 10 and 100 nM; experiments were repeated four times using cell pools from different patients. Individual experiments consisted of eight replicates. Values shown were normalized to those from untreated controls and are given as arbitrary fluorescence intensities (AU). Values observed after 2 h when the experiments were terminated were as follows (mean ± SD): 1.73 ± 0.05 for DA 10 nM and 1.86 ± 0.06 for DA 100 nM. Values at 2 h in treatment groups 10 and 100 nM DA were higher than untreated control (ANOVA, $P < 0.001$). (**B**) ROS measurements in the presence of selective DR2-/DR1-receptor agonists U-91 (1 µM) and SKF38 (1 µM). Experiments were repeated three times and each experiment consisted of eight replicates. Values observed after 2 h, when the experiments were terminated, were as follows (mean ± SD): 1.03 ± 0.01 for 1 µM U-91 and 0.97 ± 0.01 for 1 µM SKF38. Treatment groups U-91 and SKF38 did not differ from controls at 2 h (ANOVA, $P > 0.05$). (**C**) ROS measurements in the presence of DA (100 nM) and selective DA-uptake inhibitor Nf (10 µM). Experiments (each with eight replicates) were repeated six times using cell pools from different patients. Values observed after 2 h were as follows (mean ± SD): 1.38 ± 0.19 for DA and 0.87 ± 0.07 for DA + Nf. The treatment group 100 nM DA differed from the group DA + Nf ($P < 0.001$, ANOVA) and from control ($P < 0.001$). Group DA + Nf did not differ from control ($P > 0.05$). (**D**) An inhibitor of the DA-metabolizing enzyme MAO-B (8-(3-chlorostyryl) caffeine, 10 nM) partly blocked the action of DA (100 nM) to generate ROS. Experiments were repeated two times using cell pools from different patients, and each experiment consisted of eight replicates. Values observed after 2 h when the experiments were terminated are as follows (mean ± SD): 1.80 ± 0.29 for DA and 1.45 ± 0.27 for DA + MAO-B inhibitor. The treatment group 100 nM DA differed from DA + MAO-B inhibitor at 2 h and control (ANOVA, $P < 0.001$). (**E**) The action of DA (100 nM) on ROS is significantly blocked by 1 mM NAC, a ROS scavenger. Experiments were repeated four times using cell pools from different patients with eight replicates each. Results observed after 2 h when the experiments were terminated were as follows (mean ± SD): 1.9 ± 0.19 for DA, 0.15 ± 0.03 for DA + NAC and 1.1 ± 0.1 for NAC alone. The DA group differed from DA + NAC at 2 h and the control (ANOVA, $P < 0.001$). (**F**) ROS levels in GCs treated with 100 nM DA alone and with MAO-A inhibitor (pirlindole mesylate; 10 nM) and MAO-A(10 nM) + MAO-B inhibitor (8-(3-chlorostyryl) caffeine; 10 nM). The experiment was repeated two times using cell pools from different patients. Values observed after 2 h when the experiment was terminated were as follows (mean ± SD): 1.15 ± 0.02 for DA 100 nM, 1.1 ± 0.01 for DA + MAO-A inhibitor and 1.00 ± 0.01 for DA + MAO-A + MAO-B inhibitor. At 2 h (ANOVA), the DA + MAO-A inhibitor ($P < 0.05$), DA + MAO-A + MAO-B inhibitor ($P < 0.001$) and DA groups differed from control ($P < 0.001$). DA, dopamine; ROS, reactive oxygen species; GC, granulosa cells; Nf, nomifensine; MAO, monoamine oxidase.

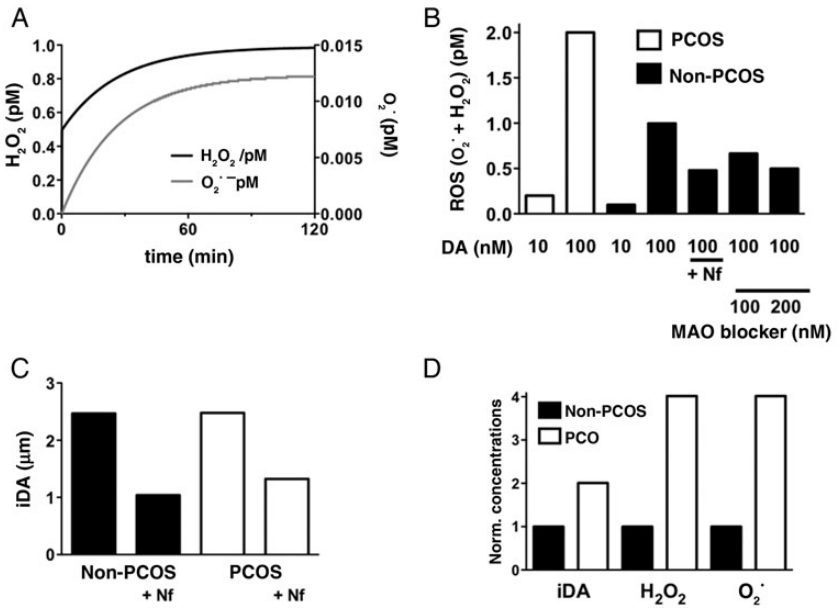

Figure 4 Computational modeling of DA uptake and metabolism. (**A**) The calculated ROS concentrations saturated at the experimental time points chosen as shown for $O_2^{\cdot-}$ and H_2O_2. (**B**) Incubation with 10 and 100 nM DA, respectively, yielded higher concentrations of ROS (sum of H_2O_2 and $O_2^{\cdot-}$) in PCOS GCs than in non-PCOS ones (as shown in the corresponding experiments depicted in Fig. 5A. The production of ROS can be blocked by either Nf or a MAO blocker. (**C**) Intracellular DA (iDA) after 2 h incubation with 5 µM DA yielded values similar to the experimental ones, and the intracellular accumulation can be blocked by Nf. (**D**) Using the extracellular DA concentrations as measured in follicular fluid (non-PCOS, 60 nM; PCOS, 120 nM) in the model yielded even higher ROS concentrations in PCOS GCs compared with non-PCOS GCs. ROS, reactive oxygen species; DA, dopamine; PCOS, polycystic ovary syndrome; MAO, monoamine oxidase; Nf, nomifensine; GC, granulosa cell.

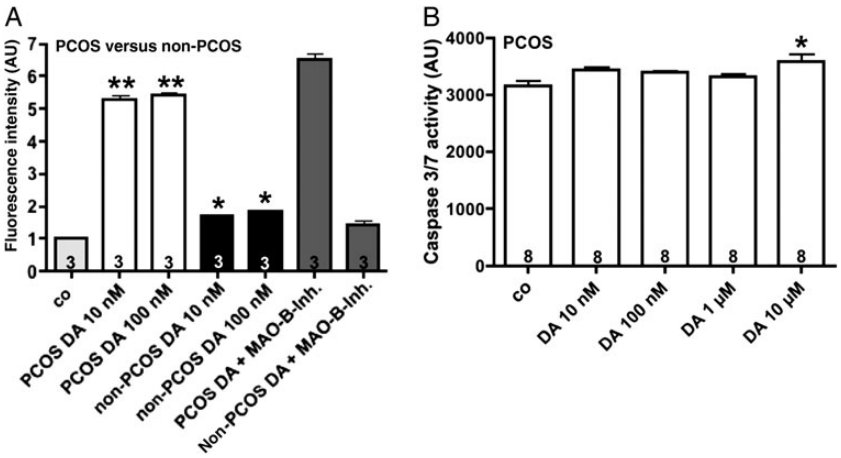

Figure 5 Comparison of increases in ROS levels induced by DA in non-PCOS versus PCOS GCs and DA influence on effector caspases 3/7 in PCOS-derived GCs. (**A**) ROS levels after 2 h in GCs from non-PCOS patients (black columns) compared with that from PCOS patients (white columns) ($n = 3$). Treatment groups with 10 and 100 nM DA differed from control. *$P < 0.05$ and **$P < 0.001$, respectively (two-way ANOVA followed by Bonferroni post-test). (**B**) Measurements of effector caspases 3/7, as an indicator for apoptosis, 24 h after DA treatment of GCs from PCOS patients. Results are expressed in arbitrary units (AU) and are mean ± SEMs from $n = 8$ experiments, each using pooled cells from 2 to 3 patients. Values with 10 µM DA are higher than the control group (*$P < 0.05$). PCOS, polycystic ovary syndrome; DA, dopamine; MAO, monoamine oxidase.

We now describe cellular uptake and metabolism of DA in human GCs, which leads to ROS production. The ability of DA to generate ROS was previously found, for example, in brain cells. In astrocytes, metabolism of DA by MAO induced the production of H_2O_2 and caused lipid peroxidation, resulting in altered Ca^{2+} signaling (Vaarmann *et al.*, 2010). Using pharmacological tools, we found that MAO-A/B and

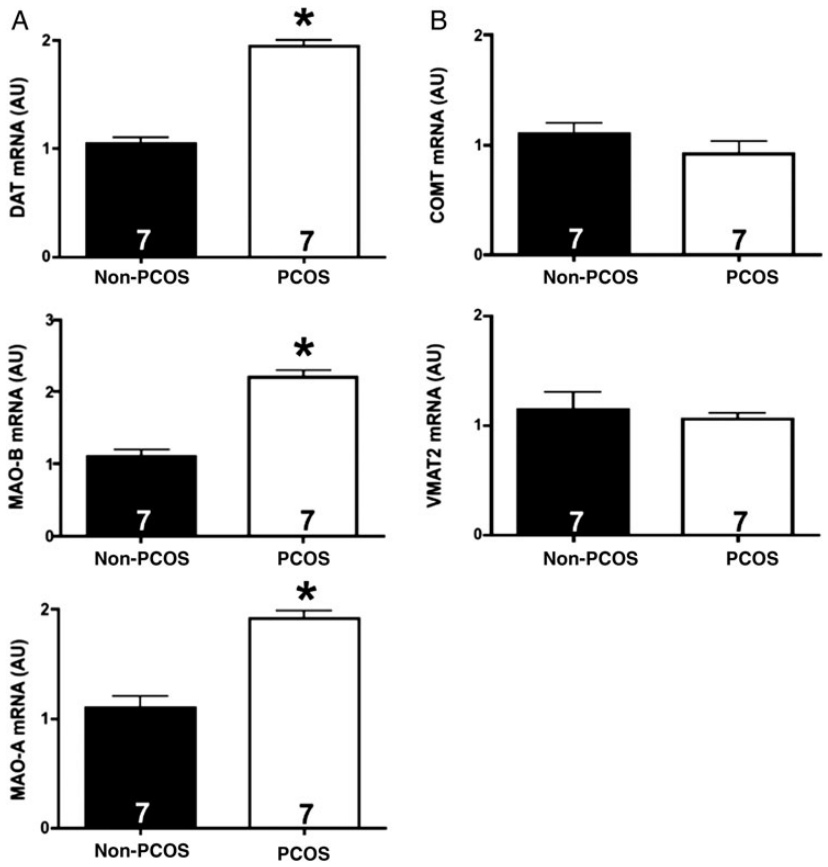

Figure 6 qRT–PCR analysis of DAT, COMT, MAO-A, -B mRNA and VMAT2 mRNA. (**A**) DAT, MAO-B and -A mRNA levels are all significantly higher in PCOS patients (mean ± SD: 1.95 ± 0.07 for DAT; 2.2 ± 0.14 for MAO-B and 1.92 ± 0.1 for MAO-A) than in non-PCOS ones (1.05 ± 0.07 for DAT; 1.1 ± 0.14 for MAO-B and 1.1 ± 0.14 for MAO-A) (*t*-test; $^*P < 0.0001$). qRT–PCR results were normalized to the housekeeping gene UQ. For all experiments, seven cell pools from 2 to 3 patients each were used. (**B**) COMT and VMAT2 mRNA expression levels of GCs do not differ significantly between PCOS (0.92 ± 0.17 for COMT and 1.06 ± 0.07 for VMAT2) and non-PCOS patients (1.1 ± 0.14 for COMT and 1.15 ± 0.21 for VMAT2) (*t*-test; $P > 0.05$). qRT–PCR results were normalized to the housekeeping gene UQ. For all experiments, seven cell pools from 2 to 3 patients each were used. DAT, dopamine transporter; COMT, catechol-*O*-methyltransferase; MAO, monoamine oxidase; VMAT, vesicular monoamine transporter.

DAT are crucially involved in DA-induced ROS generation in GCs. However, we did not find evidence for lipid peroxidation or other deleterious actions in these cells. Isoprostane levels were not increased when DA was applied in physiological and higher concentrations (data not shown) and in cell viability and caspase assays, and even supra-physiological levels of DA did not affect GCs. Are the DA-induced ROS therefore contributing to physiological processes in GCs and the ovary?

The view that ROS can be important physiological signal molecules of cells was proposed by Finkel (2011) and, indeed, this may be of special relevance for ovarian physiology. Recent observations in rodents strongly suggest that ROS are necessary for ovulatory events, including cumulus expansion and LH-induced progesterone production by pre-ovulatory follicles. ROS scavengers blocked ovulation and ROS in GCs were found to act as mediators of LH, epidermal growth factor and MAPK signaling, implicating an important role of redox signaling in the ovary, at least in rodents (Finkel, 2011; Shkolnik *et al.*, 2011; Agarwal *et al.*, 2012).

The computational modeling which we developed for GCs indicated that ROS levels in GCs depend on several factors, including the DA concentrations in follicular fluid, DA uptake and levels of metabolizing enzymes in GCs. The predictions of the model were testable in samples derived from patients with PCOS. Thus, (i) we found elevated DA levels in follicular fluid from PCOS patients. Although the sources of DA in follicular fluid are unknown, higher levels in PCOS patients may be in line with sympathetic hyper-innervation of the ovary, considered typical for PCOS (Heider *et al.*, 2001; Greiner *et al.*, 2005). However, circulating DA as a source must also be considered. Another change was observed in PCOS GCs and interestingly, (ii) the transcript levels of DAT and MAO-A/B in GCs were significantly (about 2-fold) increased. The levels of COMT (membrane-bound metabolizing enzyme) and VMAT2 (which takes up DA into vesicles and thereby prevent metabolism) were not changed. The alterations were observed in GCs cultured for several days, thus rending possible *in vivo* effects rather unlikely and imply that they may be typical for PCOS. The assumption of an increased ability of PCOS-derived human GCs to metabolize DA is supported by the results presented in a recent study, in which higher levels of DA metabolite were measured in GC cultures from PCOS than in non-PCOS patients when challenged with DA

(Gómez and Ferrero, 2011). Evidence for alterations in catecholamine metabolism together with altered mitochondrial functions in human PCOS also stem from other studies (Nemeroff and Bissette, 1988; Garcia-Rudaz *et al.*, 1998; Victor *et al.*, 2009) and are in support of our data. Finally, (iii) the computational model which we developed predicts that a higher DA metabolism leads to increased generation of ROS. Indeed, in our experiments, we observed in PCOS GCs a strikingly altered response to DA. Thus, when challenged with DA, the induced ROS levels were more than 4-fold increased over those found in non-PCOS GCs. The study of GCs from PCOS patients also revealed that the application of supra-physiological concentrations of DA can lead to a small but statistically significant increase of active caspase 3/7, indicating increased apoptosis and presumably oxidative stress. Clearly, the concentration of DA necessary to induce this action was much higher than the highest one found in our measurements of follicular fluid, and thus, the *in vivo* relevance of this results remains to be proven. Yet, DA is not the only factor increasing ROS in human GCs. Such actions were recently found for NE and decorin, acting via epidermal growth factor receptors (Adam *et al.*, 2012a; Saller *et al.*, 2012). It remains to be shown whether the actions of different ROS-elevating signaling factors may be additive and could explain the observed overall increase in ROS and the resulting oxidative stress in ovarian pathologies, including PCOS. Excessive ROS in the follicle is linked to impaired oocyte maturation and fertilization, poor embryo quality and decreased pregnancy rates (Ruder *et al.*, 2008; Bausenwein *et al.*, 2010; Chattopadhayay *et al.*, 2010; Pandey *et al.*, 2010; Qiao and Feng, 2011; Insenser *et al.*, 2013; Karuputhula *et al.*, 2013) and is an important contributing factor in PCOS.

In summary, the study identifies DA as a factor in human follicular fluid and shows that mechanisms for cellular uptake and metabolism of DA, known from the nervous system, exist in GCs of the human ovary. The results suggest that DA is a player in the human ovarian follicle, which in a receptor-independent way appears to contribute to ROS homeostasis in the follicular microenvironment. Changes in DA levels, uptake or metabolism, including the observed alterations associated with PCOS, may significantly modify the ovarian actions of DA and via ROS may contribute to the impairments of ovarian functions seen in PCOS.

Supplementary data

Supplementary data are available at http://humrep.oxfordjournals.org/.

Acknowledgements

We gratefully acknowledge the skillful help of Daniel Einwang, Astrid Tiefenbacher, Sandra Raffael and the support by Karin Metzrath.

Authors' roles

S.S. performed the majority of the experiments and analyzed the results. L.K. contributed to the work with the computational model. H.L. and J.U. contributed by performing HPLC studies. D.B., U.B., C.J.T., S.H. and R.P. contributed essential human GCs and follicular fluid and provided important conceptual input. A.M. conceived of the study and designed the research. Together with S.S., he directed the work and drafted the manuscript. All authors contributed to the final version of the paper and approved it.

Funding

This work was supported by a grant from DFG MA1080/17-3 and in part MA1080/19-1.

Conflict of interest

None declared.

References

Acharya U, Small J, Randall J, Hamilton M, Templeton A. Prospective study of short and long regimens of gonadotropin-releasing hormone agonist in in vitro fertilization program. *Fertil Steril* 1992;**57**:815–818.

Adam M, Saller S, Ströbl S, Hennebold JD, Dissen GA, Ojeda SR, Stouffer RL, Berg D, Berg U, Mayerhofer A. Decorin is a part of the ovarian extracellular marix in primates and may act as a signaling molecule. *Hum Reprod* 2012a; **27**:3249–3258.

Adam M, Urbanski HF, Garyfallou VT, Welsch U, Köhn FM, Schwarzer UJ, Strauss L, Poutanen M, Mayerhofer A. High levels of the extracellular matrix proteoglycan decorin are associated with inhibition of testicular function. *Int J Androl* 2012b;**35**:550–561.

Agarwal A, Aponte-Mellado A, Premkumar BJ, Shaman A, Gupta S. The effects of oxidative stress on female reproduction: a review. *Reprod Biol Endocrinol* 2012;**10**:49.

Anesetti G, Lombide P, D'Albora H, Ojeda SR. Intrinsic neurons in the human ovary. *Cell Tissue Res* 2001;**306**:231–237.

Bausenwein J, Serke H, Eberle K, Hirrlinger J, Jogschies P, Hmeidan FA, Blumenauer V, Spanel-Borowski K. Elevated levels of oxidized low-density lipoprotein and of catalase activity in follicular fluid of obese women. *Mol Hum Reprod* 2010;**16**:117–124.

Best JA, Nijhout HF, Reed MC. Homeostatic mechanisms in dopamine synthesis and release: a mathematical model. *Theor Biol Med Model* 2009;**6**:21.

Best J, Reed M, Nijhout HF. Models of dopaminergic and serotonergic signaling. *Pharmacopsychiatry* 2010;**43**:S61–S66.

Bolann BJ, Henriksen H, Ulvik RJ. Decay kinetics of $O_2^{\cdot-}$ studied by direct spectrophotometry. Interaction with catalytic and non-catalytic substances. *Biochem Biophys Acta* 1992;**1156**:27–33.

BRENDA, The Comprehensive Enzyme Information System, Prof. Dr. D. Schomburg, Institut fuer Biochemie und Bioinformatik, Technische Universität Braunschweig, Langer Kamp 19B 38106 Braunschweig, Germany. http://www.brenda-enzymes.de/.

Chattopadhayay R, Ganesh A, Samanta J, Jana SK, Chakravarty BN, Chaudhury K. Effect of follicular fluid oxidative stress on meiotic spindle formation in infertile women with polycystic ovarian syndrome. *Gynecol Obstet Invest* 2010;**69**:197–202.

Chen N, Justice JB. Differential effect of structural modification of human dopamine transporter on the inward and outward transport of dopamine. *Brain Res Mol Brain Res* 2000;**75**:208–215.

Chen JF, Steyn S, Staal R, Petzer JP, Xu K, Van Der Schyf CJ, Castagnoli K, Sonsalla PK, Castagnoli N Jr, Schwarzschild MA. 8-(3-Chlorostyryl) caffeine may attenuate MPTP neurotoxicity through dual actions of monoamine oxidase inhibition and A2A receptor antagonism. *J Biol Chem* 2002;**277**:36040–36044.

Ehrmann DA. Polycystic ovary syndrome. *N Engl J Med* 2005; **352**:1223–1236.

Eisenhofer G, Aneman A, Hooper D, Holmes C, Goldstein DS, Friberg P. Production and metabolism of dopamine and norepinephrine in mesenteric organs and liver of swine. *Am J Physiol* 1995;**268**:G641–G649.

Fernández de Arriba A, Lizcano JM, Balsa D, Unzeta M. Contribution of different amine oxidases to the metabolism of dopamine in bovine retina. *Biochem Pharmacol* 1991;**42**:2355–2361.

Finkel T. Signal transduction by reactive oxygen species. *J Cell Biol* 2011; **194**:7–15.

Garcia-Rudaz C, Armando I, Levin G, Escobar ME, Barontini M. Peripheral catecholamine alterations in adolescents with polycystic ovary syndrome. *Clin Endocrinol (Oxf)* 1998;**49**:221–228.

Goldstein DS, Eisenhofer G, Kopin IJ. Sources and significance of plasmalevels of catechols and their metabolites in humans. *J Pharmacol Exp Ther* 2003; **305**:800–811.

Goldstein S, Fridovich I, Czapski G. Kinetic properties of Cu,Zn-superoxide dismutase as a function of metal content—order restored. *Free Radic Biol Med* 2006;**41**:937–941.

Gómez R, Ferrero H, Delgado-Rosas F, Gaytan M, Morales C, Zimmermann RC, Simón C, Gaytan F, Pellicer A. Evidences for the existence of a low dopaminergic tone in polycystic ovarian syndrome: implications for OHSS development and treatment. *J Clin Endocrinol Metab* 2011;**96**:2484–2492.

Greiner M, Paredes A, Araya V, Lara HE. Role of stress and sympathetic innervation in the development of polycystic ovary syndrome. *Endocrine* 2005;**28**:319–324.

Greiner M, Paredes A, Rey-Ares V, Saller S, Mayerhofer A, Lara HE. Catecholamine uptake, storage, and regulated release by ovarian granulosa cells. *Endocrinology* 2008;**149**:4988–4996.

Gu H, Wall SC, Rudnick G. Stable expression of biogenic amine transporters reveals differences in inhibitor sensitivity, kinetics, and ion dependence. *J Biol Chem* 1994;**269**:7124–7130.

Heider U, Pedal I, Spanel-Borowski K. Increase in nerve fibers and loss of mast cells in polycystic and postmenopausal ovaries. *Fertil Steril* 2001; **75**:1141–1147.

Hoops S, Sahle S, Gauges R, Lee C, Pahle J, Simus N, Singhal M, Xu L, Mendes P, Kummer U. COPASI—a COmplex PAthway SImulator. *Bioinformatics* 2006;**22**:3067–3074.

Houslay MD, Tipton KF. A kinetic evaluation of monoamine oxidase activity in rat liver mitochondrial outer membranes. *Biochem J* 1974;**139**:645–652.

Insenser M, Montes-Nieto R, Murri M, Escobar-Morreale HF. Proteomic and metabolomic approaches to the study of polycystic ovary syndrome. *Mol Cell Endocrinol* 2013;**370**:65–77.

Justice JB Jr, Nicolaysen LC, Michael AC. Modeling the dopaminergic nerve terminal. *J Neurosci Methods* 1988;**22**:239–252.

Karuputhula NB, Chattopadhyay R, Chakravarty B, Chaudhury K. Oxidative status in granulosa cells of infertile women undergoing IVF. *Syst Biol Reprod Med* 2013;**59**:91–98.

Kowald A, Lehrach H, Klipp E. Alternative pathways as mechanism for the negative effects associated with overexpression of superoxide dismutase. *J Theor Biol* 2006;**238**:828–840.

Lara HE, Porcile A, Espinoza J, Romero C, Luza SM, Fuhrer J, Miranda C, Roblero L. Release of norepinephrine from human ovary: coupling to steroidogenic response. *Endocrine* 2001;**15**:187–192.

Lingjaerde O, Kildemo O. Dopamine uptake in platelets: two different low-affinity, saturable mechanisms. *Agents Actions* 1981;**11**:410–416.

Mayerhofer A, Smith GD, Danilchik M, Levine JE, Wolf DP, Dissen GA, Ojeda SR. Oocytes are a source of catecholamines in the primate ovary: evidence for a cell-cell regulatory loop. *Proc Natl Acad Sci USA* 1998; **95**:10990–10995.

Mayerhofer A, Hemmings HC Jr, Snyder GL, Greengard P, Boddien S, Berg U, Brucker C. Functional dopamine-1 receptors and DARPP-32 are expressed in human ovary and granulosa luteal cells in vitro. *J Clin Endocrinol Metab* 1999;**84**:257–264.

Mayerhofer A, Fritz S, Grünert R, Sanders SL, Duffy DM, Ojeda SR, Stouffer RL. D1-Receptor, DARPP-32, and PP-1 in the primate corpus luteum and luteinized granulosa cells: evidence for phosphorylation of DARPP-32 by dopamine and human chorionic gonadotropin. *J Clin Endocrinol Metab* 2000;**85**:4750–4757.

Mayerhofer A, Fritz S, Mani S, Rajendra Kumar T, Thalhammer A, Ingrassia P, Fienberg AA, Greengard P. Ovarian function and morphology after deletion of the DARPP-32 gene in mice. *Exp Clin Endocrinol Diabetes* 2004;**112**:451–457.

Missale C, Nash SR, Robinson S, Jaber M, Caron MG. Dopamine: from structure to function. *Physiol Rev* 1998;**78**:189–225.

Nemeroff CB, Bissette G. Neuropeptides, dopamine, and schizophrenia. *Ann NY Acad Sci* 1988;**537**:273–291.

Nicolaysen LC, Justice JB Jr. Effects of cocaine on release and uptake of dopamine in vivo: differentiation by mathematical modeling. *Pharmacol Biochem Behav* 1988;**31**:327–335.

O'Carroll AM, Bardsley ME, Tipton KF. The oxidation of adrenaline and noradrenaline by the two forms of monoamine oxidase from human and rat brain. *Neurochem Int* 1986;**8**:493–500.

Pandey AN, Tripathi A, PremKumar KV, Shrivastav TG, Chaube SK. Reactive oxygen and nitrogen species during meiotic resumption from diplotene arrest in mammalian oocytes. *J Cell Biochem* 2010;**111**:521–528.

Perfeito R, Cunha-Oliveira T, Rego AC. Revisiting oxidative stress and mitochondrial dysfunction in the pathogenesis of Parkinson disease-resemblance to the effect of amphetamine drugs of abuse. *Free Radic Biol Med* 2012;**53**:1791–1806.

Petzer JP, Steyn S, Castagnoli KP, Chen JF, Schwarzschild MA, Van der Schyf CJ, Castagnoli N. Inhibition of monoamine oxidase B by selective adenosine A2A receptor antagonists. *Bioorg Med Chem* 2003; **11**:1299–1310.

Qiao J, Feng HL. Extra- and intra-ovarian factors in polycystic ovary syndrome: impact on oocyte maturation and embryo developmental competence. *Hum Reprod Update* 2011;**17**:17–33.

Qi Z, Miller GW, Voit EO. Computational systems analysis of dopamine metabolism. *PLoS One* 2008;**3**:e2444.

Rey-Ares V, Lazarov N, Berg D, Berg U, Kunz L, Mayerhofer A. Dopamine receptor repertoire of human granulosa cells. *Reprod Biol Endocrinol* 2007;**5**:40.

Revised 2003 consensus on diagnostic criteria and long-term health risks related to polycystic ovary syndrome (PCOS). *Hum Reprod* 2004; **19**:41–47.

Riley DP, Rivers WJ, Weiss RH. Stopped-flow kinetic analysis for monitoring superoxide decay in aqueous systems. *Anal Biochem* 1991;**196**:344–349.

Ruder EH, Hartman TJ, Blumberg J, Goldman MB. Oxidative stress and antioxidants: exposure and impact on female fertility. *Hum Reprod Update* 2008;**14**:345–357.

Saller S, Kunz L, Dissen GA, Stouffer R, Ojeda SR, Berg D, Berg U, Mayerhofer A. Oxytocin receptors in the primate ovary: molecular identity and link to apoptosis in human granulosa cells. *Hum Reprod* 2010;**25**:969–976.

Saller S, Merz-Lange J, Raffael S, Hecht S, Pavlik R, Thaler C, Berg D, Berg U, Kunz L, Mayerhofer A. Norepinephrine, active norepinephrine transporter, and norepinephrine metabolism are involved in the generation of reactive oxygen species in human ovarian granulosa cells. *Endocrinology* 2012;**153**:1472–1483.

Schell C, Albrecht M, Spillner S, Mayer C, Kunz L, Koehn FM, Schwarzer U, Mayerhofer A. 15-Deoxy-delta 12–14-prostaglandin-J2 induces hypertrophy and loss of contractility in human testicular peritubular cells: implications for human male fertility. *Endocrinology* 2010;**151**:1257–1268.

Shkolnik K, Tadmor A, Ben-Dor S, Nevo N, Galiani D, Dekel N. Reactive oxygen species are indispensable in ovulation. *Proc Natl Acad Sci USA* 2011;**108**:1462–1467.

Stener-Victorin E, Jedel E, Janson PO, Sverrisdottir YB. Low frequency electroacupuncture and physical exercise decrease high muscle

sympathetic nerve activity in polycystic ovary syndrome. *Am J Physiol Regul Integr Comp Physiol* 2009;**297**:R387–R395.

Sulzer D, Schmitz Y. Parkinson's disease: return of an old prime suspect. Parkinson's disease: return of an old prime suspect. *Neuron* 2007;**55**:8–10.

Surmeier DJ. Calcium, ageing, and neuronal vulnerability in Parkinson's disease. *Lancet Neurol* 2007;**6**:933–938.

Vaarmann A, Gandhi S, Abramov AY. Dopamine induces Ca^{2+} signaling in astrocytes through reactive oxygen species generated by monoamine oxidase. *J Biol Chem* 2010;**285**:25018–25023.

Van Loon GR. Plasma dopamine: regulation and significance. *Fed Proc* 1983; **42**:3012–3018.

Victor VM, Rocha M, Bañuls C, Sanchez-Serrano M, Sola E, Gomez M, Hernandez-Mijares A. Mitochondrial complex I impairment in leukocytes from polycystic ovary syndrome patients with insulin resistance. *J Clin Endocrinol Metab* 2009;**94**:3505–3512.

Vlok N, Malan SF, Castagnoli N Jr, Bergh JJ, Petzer JP. Inhibition of monoamine oxidase B by analogues of the adenosine A2A receptor antagonist (E)-8-(3-chlorostyryl) caffeine (CSC). *Bioorg Med Chem* 2006;**14**:3512–3521.